Method Development and Validation for the Determination of Various Sulfur-Containing Anions and Other Anions in the Corrosion Process by Capillary Ion Electrophoresis with Indirect Detection

Hairui Liang*

Purdue University, School of Pharmacy and Pharmacal Sciences, D711 Myers Building, 1001 West 10th Street, Indianapolis, IN 46202

Abstract

A method of capillary ion electrophoresis with indirect detection is developed for the simultaneous determination of the sulfur-containing anions $S_2O_4^{2-}$, $S_2O_3^{2-}$, SO_4^{2-}, SO_3^{2-}, and S^{2-} and other anions (Cl^-, Br^-, NO_2^-, NO_3^-, $(COO)_2^{2-}$, F^-, and PO_4^{3-}) in the corrosion process. The effects of pH, tetradecyltrimethylammonium hydroxide, chromate, 2-[*n*-cyclohexylamino]-ethane sulfonate, calcium gluconate, and acetonitrile on the migration and resolution of the anions and the stability of sulfur-containing anions are systematically investigated. The detection limits, repeatability, and linearity for the anions are comparatively studied at 374, 274, and 254 nm, and the results show that 374 nm is the optimal length. The simultaneous multiwavelength detection at 374, 254, 214, and 195 nm can assist in confirming the identification of UV-absorbing anions.

Introduction

In the corrosion process, various anions form from alloying elements during the dissolution of a material. The anions of interest in corrosion studies include various sulfur-containing anions ($S_2O_4^{2-}$, $S_2O_3^{2-}$, SO_4^{2-}, SO_3^{2-}, and S^{2-}) and others such as NO_2^- and NO_3^- that are originated from a corroding metal substrate as alloying elements (i.e., S and N). Much evidence has shown that alloyed sulfur ($S_2O_4^{2-}$, $S_2O_3^{2-}$, SO_4^{2-}, SO_3^{2-}, and S^{2-}) has deleterious effects on the corrosion resistance of various alloys, but the mechanism has not been unambiguously delineated. In addition, the role of Cl^-, Br^-, F^-, PO_4^{3-}, and $(COO)_2^{2-}$ in the mitigation or acceleration of the localized corrosion processes is still an object of controversy. Few methods exist for the determination of anions in corrosion-process studies. Therefore, it is necessary to develop a fast, efficient, sensitive, and reliable method for the determination of the anions in corrosion-process studies.

Traditional methods for the analysis of individual anions included time-consuming and laborious gravimetric and volumetric methods. Later on, ion chromatography became a suitable instrumental method. For the specific sulfur species, the use of optical and electrochemical methods have been known for quite a long time. However, the simultaneous and quantitative determination of the desired anions are not provided by any of these methods.

As an alternative, capillary ion electrophoresis (CIE) has recently been demonstrated to be a very promising technique for the separation of different anions because of its simplicity, speed, low operating costs, small sample size, and ease of automation (1–3). Fast separations of anions are achieved when the capillary wall is coated with a surfactant such as tetradecyltrimethylammonium hydroxide (TTAOH), thus causing the electro-osmotic flow to reverse. The use of chromate as both the electrolyte and UV-absorbing probe for the separation and indirect detection of inorganic anions is commonplace in CIE because of its excellent UV-absorbance characteristics and its high mobility that matches the mobility of many inorganic anions. The technique has successfully been applied to the analysis of a variety of anionic solutes in complex sample matrices, including environmental samples (4–8), pharmaceuticals (9), and others (10–12). In addition, CIE has been applied to the analysis of inorganic anions in the paper industry (13–15). Moreover, Kelly et al. has described the analysis of disparate levels of anions having relevance to corrosion processes by direct detection (16). However, the method for the simultaneous and quantitative determination of various sulfur-containing anions ($S_2O_4^{2-}$, $S_2O_3^{2-}$, SO_4^{2-}, SO_3^{2-}, and S^{2-}) and other anions (NO_2^-, NO_3^-, Cl^-, Br^-, $(COO)_2^{2-}$, F^-, and PO_4^{3-}) has not been available.

The aim of this study was to establish a fast, efficient, sensitive, and reliable method for the simultaneous and quantitative determination of various sulfur anions and other anions in corrosion processes. In order to reach this aim, the experimental parameters for the determination of various sulfur anions and other anions were first optimized. Then, the devel-

* Author to whom correspondence should be addressed: e-mail hailiang@iupui.edu.

oped method was further validated for the sensitivity, precision, linearity, and stability of the anions. Finally, the validated method was applied to the quantitative analysis of the anions in corrosion processes.

Experimental

Chemicals

All chemicals were of analytical-reagent grade. NaH_2PO_4•$2H_2O$, NaH_2PO_4•$2H_2O$, $Na_2S_2O_3$•$5H_2O$, Na_2SO_4, Na_2S, NaCl, NaBr, $NaNO_2$, $NaNO_3$, $Na_2(COO)_2$, NaOH, and HCl were obtained from E. Merck (Darmstadt, Germany). $Na_2S_2O_4$, Na_2SO_3, NaF, mannitol, and Na_3PO_4 were from Aldrich (Steinheim, Germany). TTAOH (which was used as the electroosmotic flow modifier OFM-OH) was obtained from Waters (Milford, MA) (CIA-Pak OFM-OH). Na_2CrO_4•$4H_2O$, calcium gluconate, and 2-[*n*-cyclohexylamino]-ethane sulfonate (CHES) were obtained from Sigma (St. Louis, MO), and acetonitrile was from Rathburn Chemicals (Walkerburn, U.K.).

Apparatus and procedure

The separations were performed on a Hewlett-Packard (Avondale, PA) Chemstation 3D capillary electrophoresis equipped with an HP diode-array detector (DAD) and an air-cooling system for the capillary cassette (Hewlett-Packard). The dimensions of the fused-silica capillary (Composite Metal Services Ltd., Worcestershire, U.K.) were 60-cm (51.5-cm effective length) × 0.050-mm i.d. × 0.360-mm o.d. All experiments were carried out at 25°C and applied voltage (negative polarity) at 15 kV. Samples were introduced into a capillary from the cathodic end with 50 mbar of pressure for 5 s. All pH adjustments were made using NaOH or HCl. The electrode system was calibrated with phosphate (pH 7.00) and boric acid/potassium chloride–sodium hydroxide (pH 10.00) obtained from E. Merck.

The new capillary was flushed with 1M NaOH and H_2O successively for 10 min each. The capillary was daily conditioned by successive washing with 0.1M NaOH and water for 5 min each. Between consecutive analyses, the capillary was purged with 0.1M NaOH for 2 min and the running buffer for 5 min regularly.

Water with a conductivity of 18 MΩ generated by a Milli-Q laboratory water purification system (Millipore Corp., Bedford, MA) was used for the preparation of the electrolytes, standards, and samples. Stock solutions of approximately 1000 µg/mL of each standard sulfur anion were prepared in 10mM mannitol in order to reduce redox reaction and other inorganic anion standards in water. All sulfur anions and standard mixtures were freshly prepared every working day. Each standard anion solution (1–250 µg/mL) and the standard mixture (5–100 µg/mL) was diluted from 1000-µg/mL stock solutions of a single anion. All of the buffer solutions and standard anions and samples were filtered through 0.2-µm membrane filters. Helium degassing was necessary in order to prevent the alterations of redox sensitive species by dissolved oxygen. Analyses were performed immediately after sample preparation.

Results and Discussion

Development of method

Identification of anions

The typical UV spectra obtained for chromate and the investigated anions (sodium salts) are shown in Figures 1 and 2. It should be mentioned that the sulfide ion was actually present as HS^- at pH 9–11. Five wavelengths (374, 274, 254, 214, and 195 nm) were chosen to identify the anions and optimize the

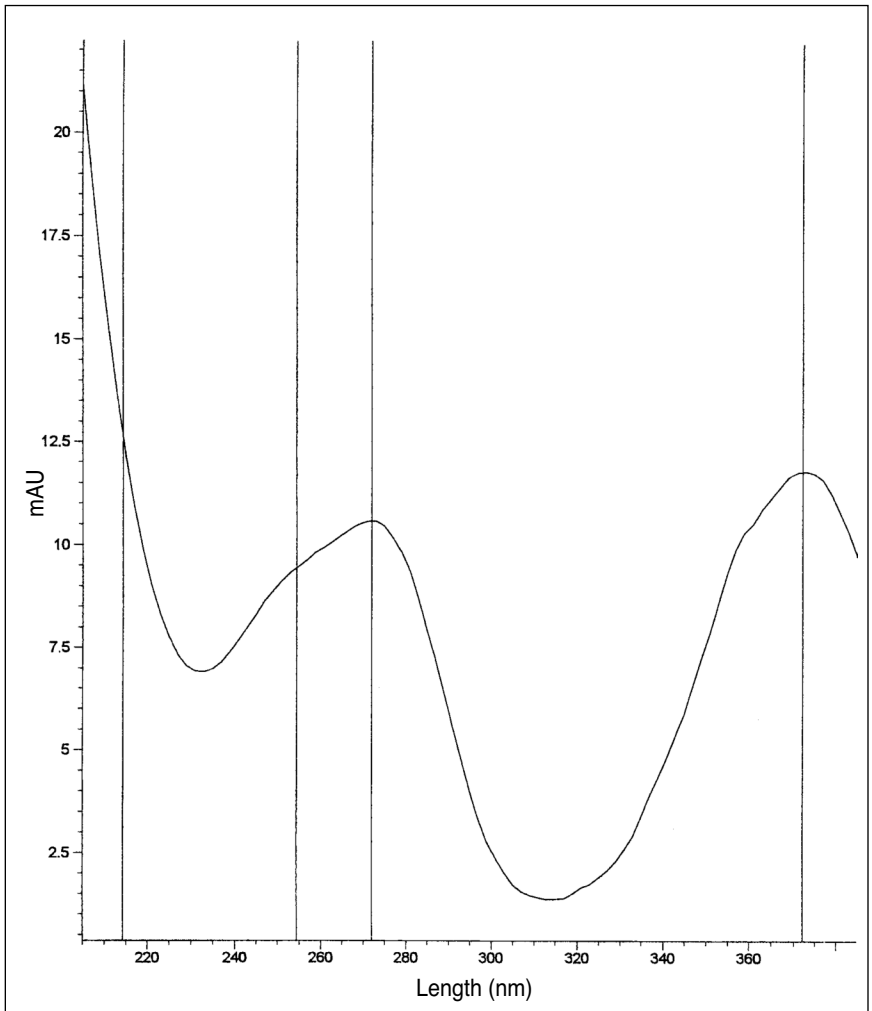

Figure 1. Typical UV spectrum obtained for Chromate (sodium salt) in the range of 195 to 400 nm. The lines superimposed on the UV spectrum represent four of the five wavelengths chosen (214, 254, 274, and 374 nm, respectively).

detection wavelength (Figures 3A–3E). At 374 and 274 nm, all anions showed positive peaks, which indicates that chromate absorbed more strongly than the anions (Figures 3A and 3B); therefore, the two wavelengths permitted universal indirect detection of all the anions. At 254 nm, only HS^- showed a negative peak (Figure 3C) because it absorbed more strongly than chromate (Figures 1 and 2). Therefore, HS^- could easily be identified at 254 nm. Also, at 214 nm, HS^-, Br^-, NO_2^-, NO_3^-, and $S_2O_3^{2-}$ showed negative peaks (Figure 3D) because they absorbed more strongly than chromate whose UV absorption was at a minimum at that wavelength. However, the peaks for SO_3^{2-}, $S_2O_4^{2-}$, and $(COO)_2^{2-}$ seemed to disappear because they absorbed as much as chromate did. Similarly, at 195 nm, Br^-, NO_2^-, HS^-, and NO_3^- still showed negative peaks, but $S_2O_3^{2-}$ showed a positive peak (Figure 3E). In addition, SO_3^{2-}, $S_2O_4^{2-}$, and $(COO)_2^{2-}$ absorbed a little bit more than chromate, showing weak positive peaks. The wavelengths at 214 and 195 nm did not permit universal indirect detection, but aided in confirming peak identity for UV-absorbing anions. Thus, the simultaneous DAD detection at 374, 254, 214, and 195 nm can help identify the UV-absorbing anions based on the peak sign (positive or negative) and the relative peak signal intensity (Table I, Figures 3A–3E). This method is very practical for accurately identifying the separated anions, because the identification of the anions is sometimes not reliable when attempted only through the comparison of migration times and by spiking with individual standards.

Optimization of detection wavelength

The length usually chosen for the indirect detection of anions when chromate is used as the visualizing reagent is 254 nm (1,4,6–15,17–18). However, there were UV maxima for chromate at 274 and 374 nm, but not at 254 nm (Figure 1). It was significant to determine which one of the three wavelengths (374, 274, and 254 nm) was optimal for the indirect detection of the anions. Consistent with the UV spectrum of chromate (Figure 1), 374 nm produced the largest signal for all the anions, and 274 nm and 254 nm had the second and third largest signals for the anions, respectively (Table I). Large detector signals alone do not always provide the most sensitivity, thus the detection limits (defined as 3 times the baseline noise) at the three wavelengths were further investigated. The results showed that 374 nm provided the best detection limits for all anions, and 274 nm and 254 nm produced the second and third best limits, respectively (Table II). Thus far, we can conclude that the DAD detector was most sensitive for all the anions at 374 nm, the next most sensitive at 274 nm, and last at 254 nm. This is not only based on the signal intensity, but also on the detection limits.

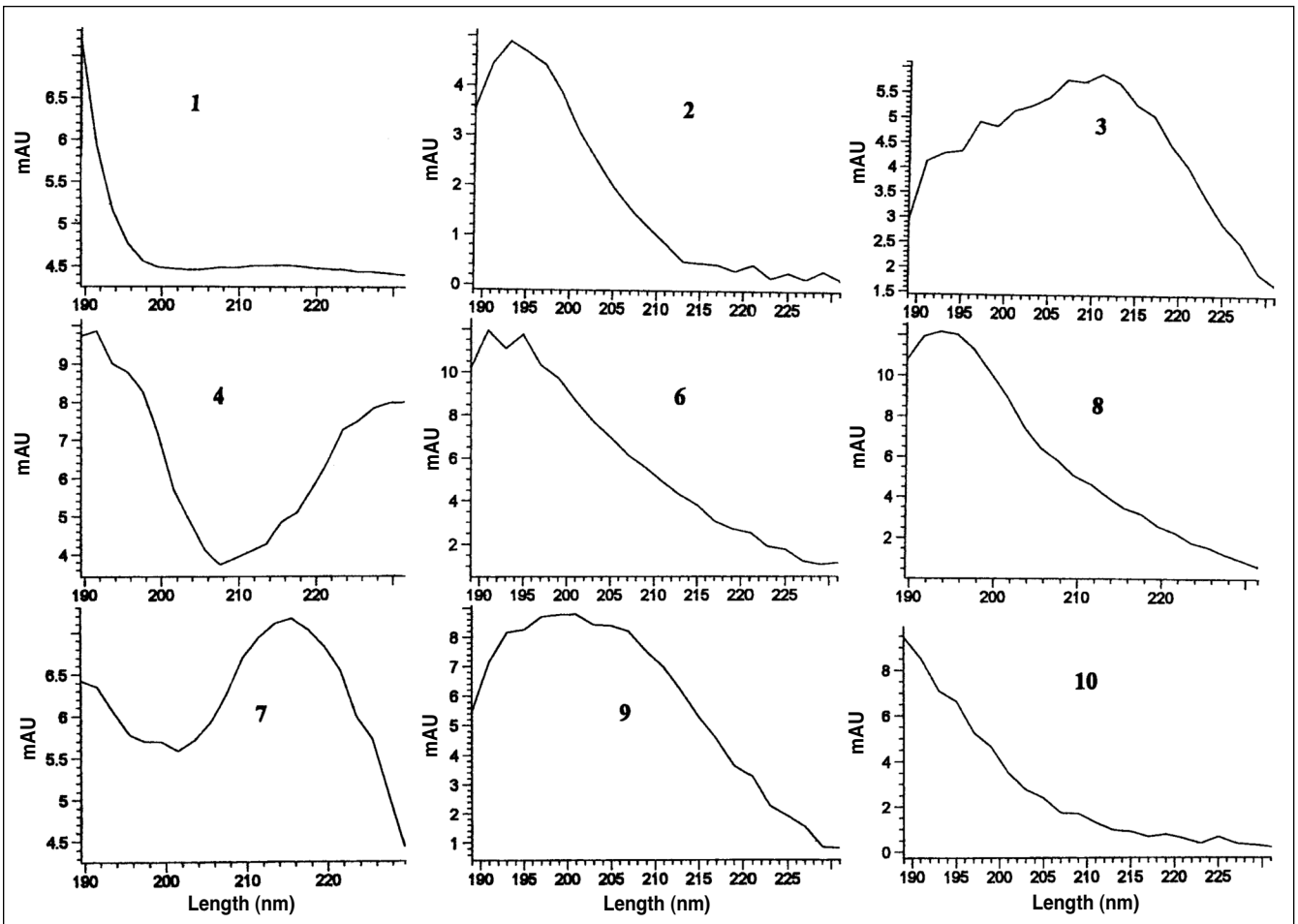

Figure 2. Typical UV spectra obtained for the investigated nine anions (sodium salt) in the range of 190 to 230 nm: Cl^-, 1; Br^-, 2; NO_2^-, 3; HS^-, 4; NO_3^-, 6; $S_2O_3^{2-}$, 7; SO_3^{2-}, 8; $S_2O_4^{2-}$, 9; and $(COO)_2^{2-}$, 10.

Effect of TTAOH concentrations

For high-speed separation of anions, TTAOH was added to the running electrolyte in order to reverse electrostatic flow (EOF). A concentration of TTAOH greater than 0.3mM in the running electrolyte is usually needed to reverse the EOF. The effect of TTAOH concentrations (0.5, 1, 2, 3, 4, and 5mM) was investigated on the separation of the anions (Figure 4). It should be noted that the strongest effect of the TTAOH concentrations was on the migration of $S_2O_3^{2-}$. Its migration time relative to Cl^- rapidly increased when TTAOH was increased because of its hydrophobicity and the formation of micelles in the running electrolyte system. Surprisingly, the effect of TTAOH did not however have much influence on the migration of HS^- as expected. As shown in Figures 5 and 6, the effect of TTAOH strongly affected the migration order and resolution of the anions. The better resolution for the successively eluted analyte pairs was achieved at 4mM TTAOH (Figure 6). The resolution (R) for the successively eluted analyte pairs was calculated as:

$$R = 2(MT_2 - MT_1)/(w_1^{1/2} + w_2^{1/2}) \quad \text{Eq. 1}$$

where MT_1 and MT_2 are the migration times and $w_1^{1/2}$ and $w_2^{1/2}$ are the peak widths of the successively eluted peaks 1 and 2, respectively.

Effect of electrolyte pH

The migration rate of a solute ion is directly proportional to its net charge, and the charge on the solute depends predominantly on the pH of the electrolyte system. Thus, pH variation is a crucial parameter for the manipulation of anion separation selectivity. The pH also governs the ionization of the visualizing reagent chromate, and high pH is needed in order for chromate to ionize fully. With the background electrolyte containing 4mM TTAOH and 5mM chromate, at pH < 9.5 the electrolyte system became opaque because of the formation of sparingly soluble chromate–TTAOH species (18). Precipitates did not form at pH < 9.5 for TTAOH or chromate when present individually, which suggests that the observed precipitate involved both species. The addition of CHES (pK_a 9.50) to the background electrolyte resulted in redissolving the precipitate,

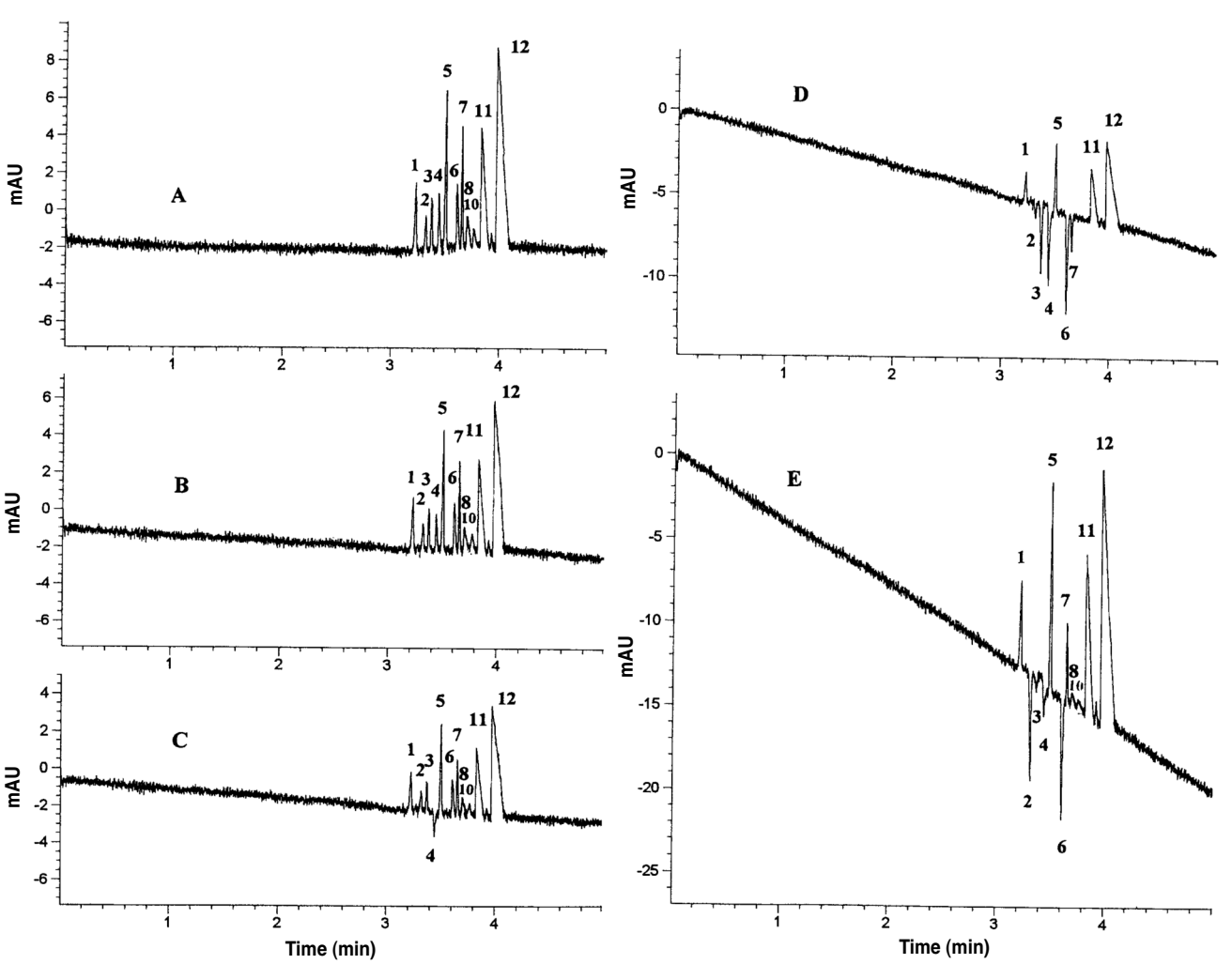

Figure 3. Electrophoregrams of a mixture of twelve standard anions with simultaneous DAD detection at (A) 374, (B) 274, (C) 254, (D) 214, and (E) 195 nm. Anions are represented as follows: Cl^-, 1; Br^-, 2; NO_2^-, 3; HS^-, 4; SO_4^{2-}, 5; NO_3^-, 6; $S_2O_3^{2-}$, 7; SO_3^{2-}, 8; $S_2O_4^{2-}$, 9; $(COO)_2^{2-}$, 10; F^-, 11; and PO_4^{3-}, 12.

even at pH values as low as 8.5. Moreover, the addition of CHES maintained constant pH in the pH ranges from 9 to 11, which was very important for the generation of stable EOF and good precision for the anions.

The effect of pH (9.0, 9.5, 10.0, 10.5, and 11.0) was first investigated in order to optimize the selectivity of the separation. As shown in Figure 7, the pH values did not affect most of the anions because of their being fully charged at the pH values, and the pH changes mainly influenced the migration of $S_2O_3^{2-}$. When increasing the pH from 9.0 to 10.5, the migration speed of $S_2O_3^{2-}$ relative to Cl^- increased continually and then decreased from pH 10.5 to 11.0, thus resulting in the change of the migration order of analytes (Figure 8).

In the five pH values, pH 10.0 seemed to be optimal, but the separation windows at pH 9.0 and 9.5 were bigger than that at pH 10.0 (Figure 7). In order to increase the resolution for the anions, the pH (9.1, 9.2, 9.3, 9.4, 9.5, and 9.6) was carefully optimized further. As shown in Figure 9, pH 9.4 was optimal. The resolution at this pH was better than that at pH 10.0, partly because of the increase of the separation window (Figure 10).

Table I. Peak Height Ratio with Respect to 374 nm at Five Different Wavelengths Using a Twelve-Anion Mixture

	Detection wavelength (nm)				
Anions	**374**	**274**	**254***	**214***	**195***
Peak height ratio					
Cl^-	1.00	0.75	0.54	0.57	1.48
Br^-	1.00	0.75	0.53	–0.57	–3.71
NO_2^-	1.00	0.76	0.50	–1.60	–0.30
HS^-	1.00	0.65	–0.54	–1.62	–0.91
SO_4^{2-}	1.00	0.76	0.54	0.52	2.18
NO_3^-	1.00	0.75	0.44	–0.56	–1.21
$S_2O_3^{2-}$	1.00	0.74	0.53	–1.69	1.08
SO_3^{2-}	1.00	0.75	0.54	0.00	0.50
$S_2O_4^{2-}$	1.00	0.75	0.53	0.00	0.50
$(COO)_2^{2-}$	1.00	0.76	0.54	0.20	0.71
F^-	1.00	0.76	0.55	0.50	1.56
PO_4^{3-}	1.00	0.76	0.53	0.44	0.41

* Shows a negative peak, which indicates the analyte is more absorbing than the background electrolyte.

Table II. Detection Limits Defined as Three Times the Baseline Noise in Micrograms per Milliliter at Three Different Wavelengths

	Detection wavelengths (nm)		
Anions	**374**	**274**	**254**
Detection limit			
Cl^-	0.22	0.24	0.25
Br^-	0.34	0.39	0.45
NO_2^-	0.31	0.36	0.42
HS^-	0.55	0.78	0.92
SO_4^{2-}	0.49	0.53	0.66
$S_2O_3^{2-}$	0.45	0.50	0.54
NO_3^-	0.41	0.41	0.96
SO_3^{2-}	0.48	0.59	0.59
$S_2O_4^{2-}$	0.48	0.53	0.63
$(COO)_2^{2-}$	0.22	0.27	0.32
F^-	0.18	0.24	0.36
PO_4^{3-}	0.69	0.92	1.21

Effect of chromate, CHES, and calcium gluconate concentrations

The effect of chromate (2.5, 5, 7.5, 10, and 15mM), CHES (5, 7.5, 10, 12.5, and 15mM), and calcium gluconate (0.05, 0.075, 0.1, 0.125 and 0.15mM) were investigated in order to improve the selectivity of the anions. The effect of chromate and CHES mainly influenced the migration of $S_2O_3^{2-}$, thus resulting in the change of the migration order and selectivity (Figures 11 and 12). Generally, the resolution for the most successively eluted analyte pairs increased with increasing the concentrations of chromate mainly because of the increase of the separation

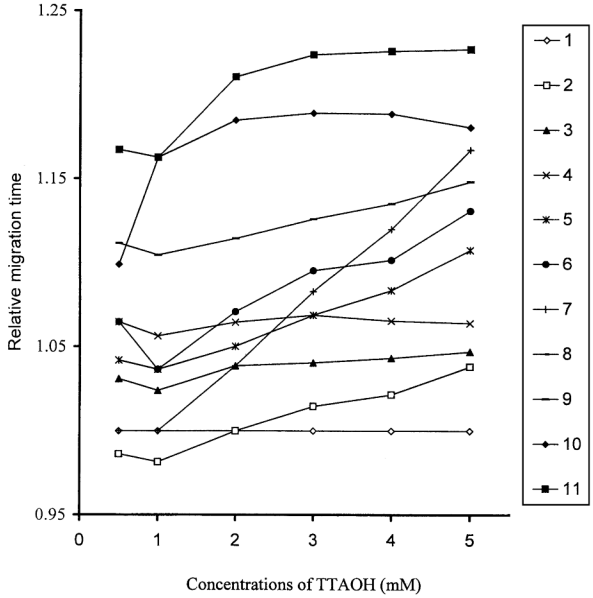

Figure 4. Relative migration times (reference anion = Cl^-) as a function of TTAOH concentrations increasing from 0.5 to 5mM: Cl^-, 1; Br^-, 2; NO_2^-, 3; HS^-, 4; SO_4^{2-}, 5; NO_3^-, 6; $S_2O_3^{2-}$, 7; SO_3^{2-}, 8; $S_2O_4^{2-}$, 9; F^-, 10; and PO_4^{3-}, 11.

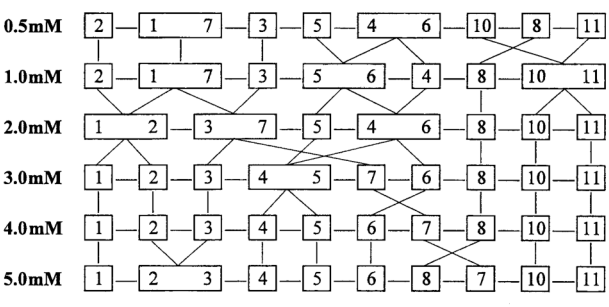

Figure 5. Migration order of the anions for increasing TTAOH concentrations from 0.5 to 5mM: Cl^-, 1; Br^-, 2; NO_2^-, 3; HS^-, 4; SO_4^{2-}, 5; NO_3^-, 6; $S_2O_3^{2-}$, 7; SO_3^{2-}, 8; $S_2O_4^{2-}$, 9; F^-, 10; and PO_4^{3-}, 11.

window. The addition of calcium gluconate mainly improved the peak shape of some anions. However, only at 5mM chromate, 10mM CHES, and 0.1mM calcium gluconate did HS^-, $S_2O_4^{2-}$, NO_3^-, and $S_2O_3^{2-}$ completely resolve, and at other concentrations some of them were overlapped (Figures 11 and 12).

Effect of acetonitrile concentrations

Acetonitrile (5, 6, 7, 8, 9, 10, 15, 20, and 25%, v/v) was added to the electrolyte system in order to improve the selectivity further. The effect of acetonitrile concentrations mainly influenced the migration of NO_3^- and $S_2O_3^{2-}$, thus resulting in the change of the migration order of the anions. For example, in the absence of acetonitrile, NO_3^- migrated faster than $S_2O_3^{2-}$ and slower than SO_4^{2-}. When 8% of the acetonitrile was added to the background electrolyte system, NO_3^- migrated faster than both. However, at 15% of acetonitrile, $S_2O_3^{2-}$ migrated much faster than NO_3^- and SO_4^{2-}. In addition, at 20 and 25%, the separation windows and resolution of the analytes greatly decreased.

After systematically investigating the effects of the previously mentioned experimental parameters on the migration of anions, the optimized buffer system was obtained as follows: 5mM Na_2CrO_4, 4mM TTAOH, 10mM CHES, and 0.1mM calcium gluconate at pH 9.4 with a detection of 374 nm. Under these conditions, eleven anions were baseline separated within 5 min (Figure 3). Interestingly, SO_3^{2-} and $S_2O_4^{2-}$ could not however be separated under any investigated conditions.

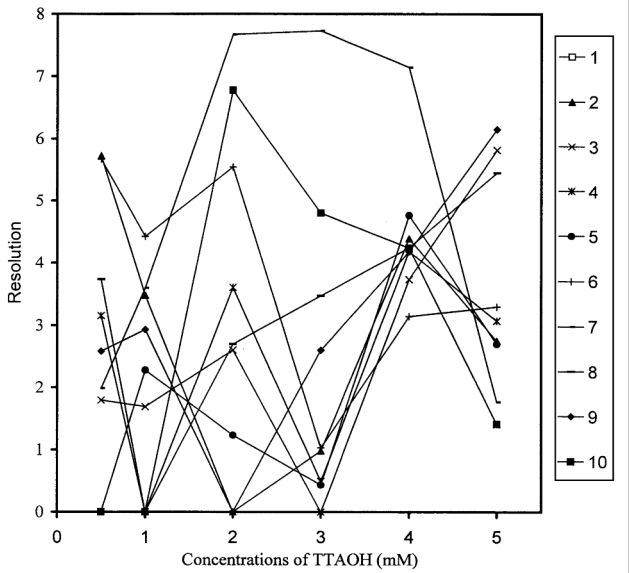

Figure 6. Effect of TTAOH concentrations from 0.5 to 5mM on the resolution of the anions. Cl^-:Br^-, 1; Br^-:NO_2^-, 2; NO_2^-:HS^-, 3; HS^-:SO_4^{2-}, 4; $S_2O_4^{2-}$:NO_4^-, 5; NO_3^-:$S_2O_3^{2-}$, 6; $S_2O_3^{2-}$:SO_3^{2-}, 7; SO_3^{2-}:$S_2O_4^{2-}$, 8; $S_2O_4^{2-}$:F^-, 9; and F^-:PO_4^{2-}, 10.

Validation of the method

The method was validated by investigating the detection

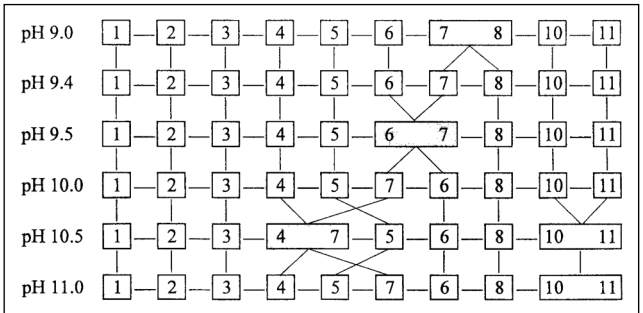

Figure 8. Migration order of the anions on increasing the pH of the background electrolyte system from 9.0 to 11.0: Cl^-, 1; Br^-, 2; NO_2^-, 3; HS^-, 4; SO_4^{2-}, 5; NO_3^-, 6; $S_2O_3^{2-}$, 7; SO_3^{2-}, 8; $S_2O_4^{2-}$, 9; F^-, 10; and PO_4^{3-}, 11.

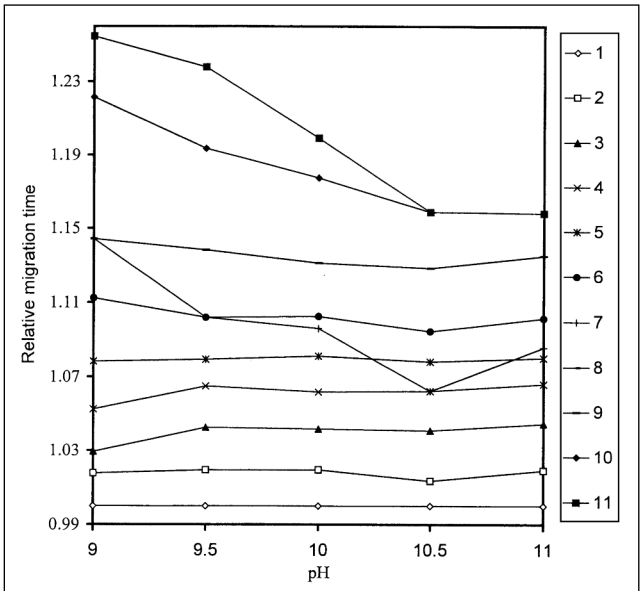

Figure 7. Relative migration times (reference anion = Cl^-) as a function of pH varied from 9.0 to 11.0: Cl^-, 1; Br^-, 2; NO_2^-, 3; HS^-, 4; SO_4^{2-}, 5; NO_3^-, 6; $S_2O_3^{2-}$, 7; SO_3^{2-}, 8; $S_2O_4^{2-}$, 9; F^-, 10; and PO_4^{3-}, 11.

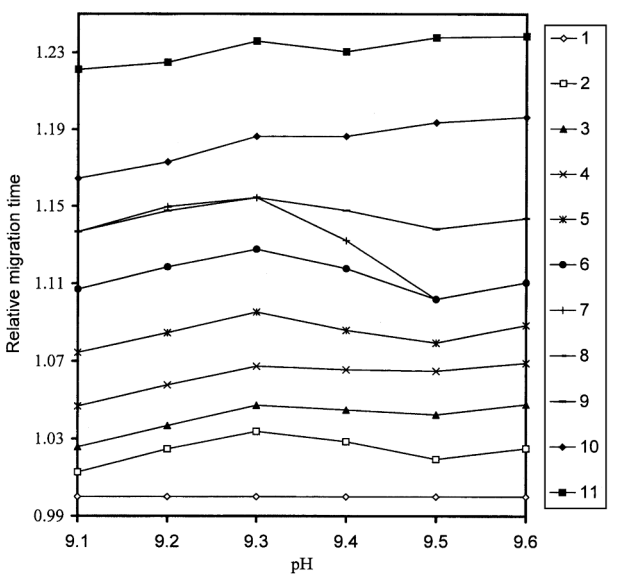

Figure 9. Relative migration times (reference anion = Cl^-) as a function of pH varied from 9.1 to 9.6: Cl^-, 1; Br^-, 2; NO_2^-, 3; HS^-, 4; SO_4^{2-}, 5; NO_3^-, 6; $S_2O_3^{2-}$, 7; SO_3^{2-}, 8; $S_2O_4^{2-}$, 9; F^-, 10; and PO_4^{3-}, 11.

limits, repeatability of analyses, and linearity for the anions at the three wavelengths of 374, 274, and 254 nm. The detection limits for all the anions were best at 374 nm, and second best at 274 nm, and last at 254 nm (Table II). In terms of migration times, the repeatability of the analysis from six replicates was approximately the same (0.13–0.58%) at all three wavelengths; whereas in terms of the corrected peak areas, the repeatability for all the anions was best at 374 nm, second best at 274 nm, and last at 254 nm (Table III). Linear ranges were wider at 374 and 274 nm for Br^-, SO_4^{2-}, $S_2O_3^{2-}$, and SO_4^{2-} than at

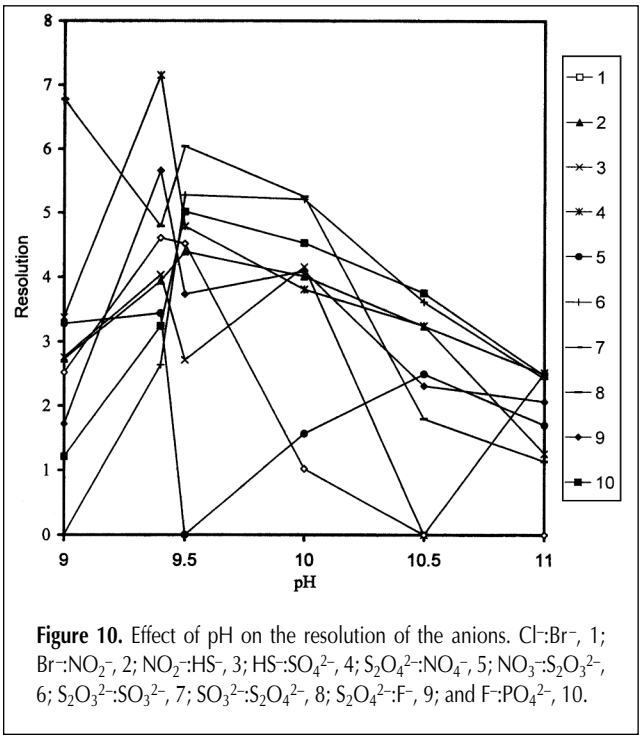

Figure 10. Effect of pH on the resolution of the anions. Cl^-:Br^-, 1; Br^-:NO_2^-, 2; NO_2^-:HS^-, 3; HS^-:SO_4^{2-}, 4; $S_2O_4^{2-}$:NO_4^-, 5; NO_3^-:$S_2O_3^{2-}$, 6; $S_2O_3^{2-}$:SO_3^{2-}, 7; SO_3^{2-}:$S_2O_4^{2-}$, 8; $S_2O_4^{2-}$:F^-, 9; and F^-:PO_4^{2-}, 10.

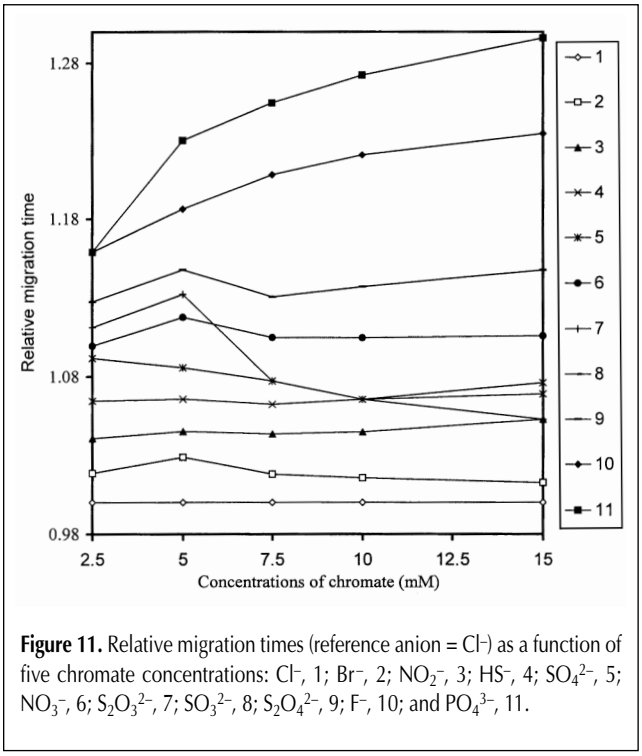

Figure 11. Relative migration times (reference anion = Cl^-) as a function of five chromate concentrations: Cl^-, 1; Br^-, 2; NO_2^-, 3; HS^-, 4; SO_4^{2-}, 5; NO_3^-, 6; $S_2O_3^{2-}$, 7; SO_3^{2-}, 8; $S_2O_4^{2-}$, 9; F^-, 10; and PO_4^{3-}, 11.

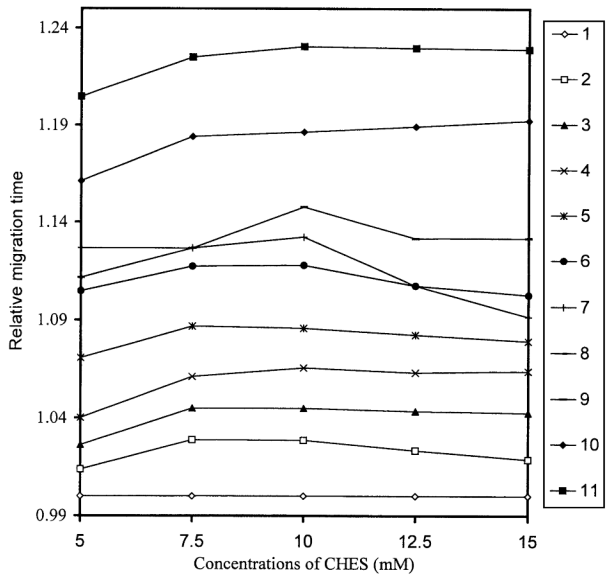

Figure 12. Relative migration times (reference anion = Cl^-) as a function of five CHES concentrations: Cl^-, 1; Br^-, 2; NO_2^-, 3; HS^-, 4; SO_4^{2-}, 5; NO_3^-, 6; $S_2O_3^{2-}$, 7; SO_3^{2-}, 8; $S_2O_4^{2-}$, 9; F^-, 10; and PO_4^{3-}, 11.

Table III. Repeatability of Analysis in Terms of Migration Times and Corrected Peak Area from Six Replicates Using the Mixture of Twelve Standard Anions at Three Different Detection Wavelengths

	Detection wavelengths (nm)		
Anions	**374**	**274**	**254**
Repeatability (RSD%) in terms of migration time			
Cl^-	0.55	0.55	0.55
Br^-	0.20	0.40	0.42
NO_2^-	0.51	0.51	0.52
HS^-	0.52	0.52	0.52
SO_4^{2-}	0.47	0.47	0.47
$S_2O_3^{2-}$	0.13	0.13	0.13
NO_3^-	0.13	0.13	0.13
SO_3^{2-}	0.57	0.57	0.57
$S_2O_4^{2-}$	0.57	0.57	0.57
$(COO)_2^{2-}$	0.55	0.55	0.55
F^-	0.58	0.57	0.58
PO_4^{3-}	0.32	0.32	0.32
Repeatability (RSD%) in terms of corrected peak area			
Cl^-	1.47	2.56	3.11
Br^-	1.26	2.72	3.47
NO_2^-	2.08	3.34	3.81
HS^-	5.13	6.21	6.21
SO_4^{2-}	1.23	0.62	5.45
$S_2O_3^{2-}$	0.79	2.27	4.65
NO_3^-	0.79	2.27	4.65
SO_3^{2-}	0.08	3.67	3.47
$S_2O_4^{2-}$	0.08	3.67	3.47
$(COO)_2^{2-}$	1.12	3.24	3.66
F^-	2.74	7.39	2.89
PO_4^{3-}	2.31	4.11	6.18

254 nm in order to obtain similar squares of the correlation coefficients (0.997–1.000 at 374 nm, 0.989–1.000 at 274 nm, and 0.984–1.000 at 254 nm) (Table IV). From the point of view of repeatability and linearity, we can also conclude that 374 nm was optimal as compared with 274 and 254 nm.

Stability of sulfur-containing anions

A measurement of 400 µg/mL $S_2O_4^{2-}$, $S_2O_3^{2-}$, SO_3^{2-}, SO_4^{2-}, or HS^- was spiked in 10mM mannitol and kept at 4°C and 20°C for 24 h in order to perform the experiment of their stability. The result showed 50% of HS^- became consumed, whereas the concentrations of $S_2O_3^{2-}$, SO_3^{2-}, and SO_4^{2-} increased significantly (Figure 13) indicating HS^- is very unstable and easily transformed into $S_2O_3^{2-}$, SO_3^{2-}, and SO_4^{2-} within a day even at 4°C. It was found that approximately 2% of SO_3^{2-} was oxygenated into SO_4^{2-}, whereas SO_4^{2-} and $S_2O_3^{2-}$ were stable. In addition, the result showed that 20% of $S_2O_4^{2-}$ became consumed when the concentrations of $S_2O_3^{2-}$ and SO_4^{2-} increased, and only less than 2% of $S_2O_4^{2-}$ was detected two weeks later. This indicated that $S_2O_4^{2-}$ was not stable even at 4°C and transformed into $S_2O_3^{2-}$ and SO_4^{2-} (Figure 14). Therefore, an immediate analysis was necessary, because some sulfur anions are redox-active species such as HS^-, $S_2O_4^{2-}$, and SO_3^{2-}. The water and mannitol solutions that are used to prepare sulfur anion samples have to be helium degassed in order to get rid of oxygen immediately prior to use.

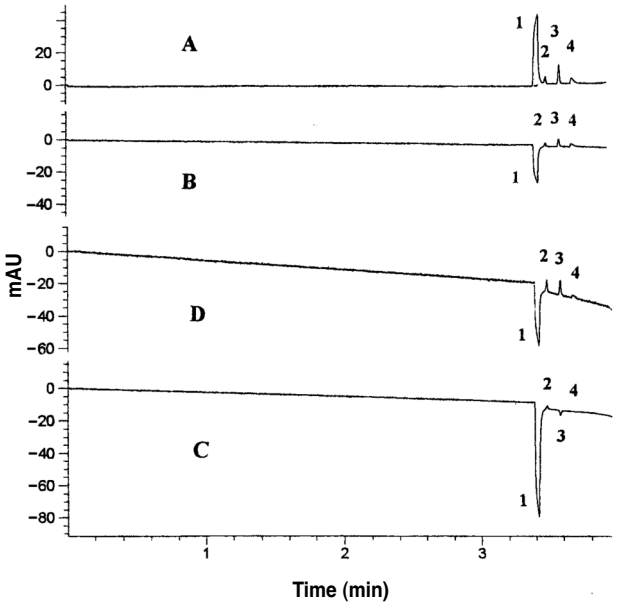

Figure 13. Electrophoregrams of HS^- with DAD detection at (A) 374, (B) 254, (C) 214, and (D) 195 nm after 400 µg/mL of HS^- was kept at 4°C for 4 h. Anions are represented as follows: HS^-, 1; SO_4^{2-}, 2; $S_2O_3^{2-}$, 3; and SO_3^{2-}, 4.

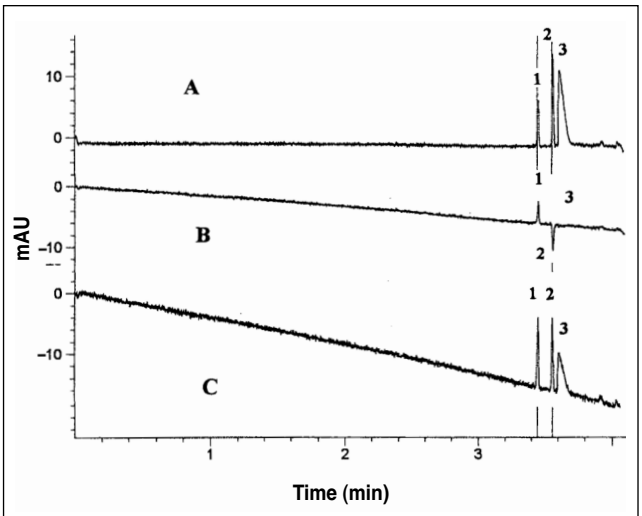

Figure 14. Electrophoregrams of $S_2O_4^{2-}$ with DAD detection at (A) 374, (B) 214, and (C) 195 nm. Anions are represented as follows: SO_4^{2-}, 1; $S_2O_3^{2-}$, 2; and $S_2O_4^{2-}$, 3.

Table IV. Linearity for the Anions at the Three Different Wavelengths*

Anions	Linear range (µg/mL)	Detection at 374 nm			Detection at 274 nm			Detection at 254 nm		
		R^2†	a‡	b§	R^2	a	b	R^2	a	b
Cl^-	1–150	0.999	0.0029	0.0111	1.000	0.0022	0.0056	0.996	0.0016	0.0054
Br^-	2.5–250	0.997	0.0009	0.0052	0.997	0.0007	0.0041	0.998**	0.0005	0.0034
NO_2^-	2.5–150	0.999	0.0010	0.0012	1.000	0.0008	0.0007	0.998	0.0006	0.0015
SO_4^{2-}	1–1000	1.000	0.0014	0.0070	1.000	0.0011	0.0072	1.000††	0.0008	0.0051
NO_3^-	1–150	0.997	0.0018	0.0061	0.989	0.0013	0.0083	0.984	0.0009	0.0078
$S_2O_3^{2-}$	2.5–150	1.000	0.0013	0.0015	1.000	0.0009	0.0022	0.999‡‡	0.0006	0.0011
$(COO)_2^{2-}$	1–150	0.998	0.0033	0.0069	0.999	0.0024	0.0050	0.998	0.0018	0.0040
$S_2O_4^{2-}$	2.5–200	0.994	0.0019	–0.0076	0.993	0.0014	–0.0058	0.992§§	0.0010	–0.0030

* Repetition number for each analysis: $n = 6$.
† R^2, square of the correlation coefficient.
‡ a, slope of the regression equation.
§ b, intercept of the regression equation.
** 5–250 µg/mL.
†† 5–1000 µg/mL.
‡‡ 5–150 µg/mL.
§§ 5–200 µg/mL.

Conclusion

A rapid, efficient, sensitive, and reliable CIE method with universal indirect detection has been developed for the separation of the anions $S_2O_3^{2-}$, SO_4^{2-}, $SO_3^{2-}/S_2O_4^{2-}$, HS^-, Cl^-, Br^-, NO_2^-, NO_3^-, $(COO)_2^{2-}$, F^-, and PO_4^{3-}. Our results have shown that with the DAD detector, 374 nm (not 254 nm) is an optimal detection wavelength for all the anions. This is not only based on the signal intensity, but also on the detection limits, repeatability, and linearity of the anions. The simultaneous multiwavelength detection at 374, 254, 214, and 195 nm can aid in confirming the peak identity of UV-absorbing anions. An immediate analysis of some sulfur-containing anions (HS^-, $S_2O_4^{2-}$, and SO_3^{2-}) is vital because of their poor stability.

References

1. P. Jandik and W.R. Jones. Optimization of detection sensitivity in the capillary electrophoresis of inorganic anions. *J. Chromatogr.* **546:** 431–44 (1991).
2. Y. Ma and R. Zhang. Optimization of indirect photometric detection in high-performance capillary electrophoresis. *J. Chromatogr.* **625:** 341–48 (1992).
3. M.P. Harrold, M.J. Wojtusik, J. Riviello, and P. Henson. Parameters influencing separation and detection of anions by capillary electrophoresis. *J. Chromatogr.* **640:** 463–71 (1993).
4. P.E. Jackson and P.R. Haddad. Optimization of injection technique in capillary ion electrophoresis for the determination of trace level anions in environmental samples. *J. Chromatogr.* **640:** 481–87 (1993).
5. R. Stahl. Routine determination of anions by capillary electrophoresis and ion chromatography. *J. Chromatogr. A* **686:** 143–48 (1994).
6. J.P. Romano and J. Krol. Capillary ion electrophoresis, an environmental method for the determination of anions in water. *J. Chromatogr.* **640:** 403–412 (1993).
7. S.A. Oehrle. Analysis of anions in drinking water by capillary ion electrophoresis. *J. Chromatogr. A* **733:** 101–104 (1996).
8. G. Bondoux, P. Jandik, and W.R. Jones. New approach to the analysis of low levels of anions in water. *J. Chromatogr.* **602:** 79–88 (1992).
9. J.B. Nair and C.G. Izzo. Anion screening for drugs and intermediates by capillary ion electrophoresis. *J. Chromatogr.* **640:** 445–61 (1993).
10. J.M. Jordan, R.L. Moese, R. Johnson–Watts, and D.E. Burton. Determination of inorganic sulfate in detergent products by capillary electrophoresis. *J. Chromatogr. A* **671:** 445–51 (1994).
11. H. Harakuwe, P.R. Haddad, and P.E. Jackson. Quantitative determination of oxalate in Bayer liquor by capillary zone electrophoresis. *J. Chromatogr. A* **739:** 399–403 (1996).
12. J.-P. Mercier, P. Morin, M. Dreux, and A. Tambute. Capillary electrophoresis analysis of chemical warfare agent breakdown products. *J. Chromatogr. A* **741:** 279–85 (1996).
13. S.M. Massselter, A.J. Zemann, and G. Bonn. Determination of inorganic anions in Kraft pulping liquors by capillary electrophoresis. *J. High Resol. Chromatogr.* **19:** 131–136 (1996).
14. D.R. Salomon and J. Romano. Applications of capillary ion electrophoresis in the pulp and paper industry. *J. Chromatogr.* **602:** 219–25 (1992).
15. D.R. Salomon and J.P. Romano. Rapid ion monitoring of Kraft process liquors by capillary electrophoresis. *Process Control and Quality* **3:** 219–27 (1992).
16. R.G. Kelly, C.S. Brossia, K.R. Cooper, and J. Krol. Analysis of disparate levels of anions of relevance to corrosion processes. *J. Chromatogr. A* **739:** 191–98 (1996).
17. W.R. Jones. Method development approaches for capillary ion electrophoresis. *J. Chromatogr.* **640:** 387–95 (1993).
18. H. Harakuwe and P.R. Haddad. Manipulation of separation selectivity for inorganic anions in capillary zone electrophoresis using control of electrolyte pH. *J. Chromatogr. A* **734:** 416–21 (1996).

Manuscript accepted September 1, 2000.